CHEMISTRY
AN ASIAN JOURNAL

DOI: 10.1002/asia.201200192

Concise Synthesis and Two-Photon-Excited Deep-Blue Emission of 1,8-Diazapyrenes

Tingchao He,[a] Pei Chui Too,[b] Rui Chen,[a] Shunsuke Chiba,*[b] and Handong Sun*[a]

Abstract: Efficient violet–blue-emitting molecules are especially useful for applications in full-color displays, solid-state lighting, as well as in two-photon absorption (TPA) excited frequency-upconverted violet–blue lasing. However, the reported violet–blue-emitting molecules generally possess small TPA cross sections. In this work, new 1,8-diazapyrenes derivatives **3** with blue two-photon-excited fluorescence emission were concisely synthesized by the coupling reaction of readily available 1,4-naphthoquinone *O*,*O*-diacetyl dioxime (**1**) with internal alkynes **2** under the $[\{RhCl_2Cp^*\}_2]$–$Cu(OAc)_2$ (Cp* = pentamethylcyclopentadienyl ligand) bimetallic catalytic system. Elongation of the π-conjugated length of 1,8-diazapyrenes **3** led to the increase of TPA cross sections without the expense of a redshift of the emission wavelength, probably due to the rigid planar structure of chromophores. It is especially noteworthy that 2,3,6,7-tetra(4-bromophenyl)-1,8-diazapyrene (**3c**) has a larger TPA cross section than those of other molecules reported so far. These experimental results are explained in terms of the effects of extension of the π-conjugated system, intramolecular charge transfer, and reduced detuning energy.

Keywords: diazapyrenes · deep-blue emission · fluorescence · nonlinear optics · two-photon absorption

Introduction

The development of efficient two-photon absorption (TPA) materials have recently been expedited by their potential applications in multiphoton microscopy, optical limiting, frequency-upconversion lasing, pulse stabilization, and reshaping.[1] To achieve large TPA cross sections, various molecular structures have been designed, such as donor–bridge–acceptor (D–π–A) dipoles,[2] donor–bridge–donor (D–π–D) quadrupoles,[3] octupoles,[4] oligomeric porphyrin derivatives,[5] and others.[6]

In addition to the aforementioned applications, TPA-induced frequency-upconverted violet–blue lasing, which can be used to generate low-cost, high-energy, coherent light sources, offers new views in various laser-based applications.[7] Moreover, violet–blue-emitting molecules have attracted much attention for their important applications, such as in full-color displays and solid-state lighting.[8] However, to the best of our knowledge, there have been only a few papers reporting the efficient two-photon-excited blue emission of organic molecules.[1]

It is generally accepted that the increase in donor–acceptor strength, the conjugation length, and the planarity of the π system will lead to large TPA cross sections.[1,9] However, the structural guidelines for enlarging TPA cross sections with violet–blue emission are extremely rare. The lack of efficient design strategies for these molecules might be a serious obstacle for their related applications. One of the structural requirements for violet–blue-emission molecules is short π conjugation, but it usually results in smaller TPA cross sections. On the other hand, elongation of π conjugation for enhancement of TPA cross section causes a redshift of the emission wavelength and decreases the fluorescence quantum yield and photostability.[10] Moreover, the TPA cross sections of violet–blue-emission molecules reported so far are very small, usually in the range of tens of GM ($1\ GM = 10^{-50}\ cm^4 s$).[11] Moreover, synthetic processes for such violet–blue-emission molecules generally require multistep routes. Based on these backgrounds, the development of concise synthetic methods for π-conjugated molecules possessing efficient two-photon-excited violet–blue emission has remained a significant challenge.

Herein, we utilize newly and concisely synthesized 1,8-diazapyrenes[12] to build up new TPA chromophores, which can efficiently emit deep-blue light. TPA cross sections, measured with femtosecond pulses by the Z-scan technique,[13] are in the range of (1–15), (6–120), (54–298), and

[a] Dr. T. He, Dr. R. Chen, Prof. H. Sun
Division of Physics and Applied Physics
School of Physical and Mathematical Sciences
Nanyang Technological University
Singapore 637371 (Singapore)
Fax: (+65) 65138086
E-mail: hdsun@ntu.edu.sg

[b] P. C. Too, Prof. S. Chiba
Division of chemistry and Biological Chemistry
School of Physical and Mathematical Sciences
Nanyang Technological University
Singapore 637371 (Singapore)
Fax: (+65) 67911961
E-mail: shunsuke@ntu.edu.sg

Supporting information for this article is available on the WWW under http://dx.doi.org/10.1002/asia.201200192.

(5–82) GM for the four 1,8-diazapyrenes **3a**, **3b**, **3c**, and **3d**, respectively (see below). Although the TPA cross sections are smaller than those of several molecules emitting at wavelengths between 500 and 700 nm, they are larger than those of most molecules with deep-blue emission.[11] Moreover, by taking the present simple preparation into consideration, 1,8-diazapyrenes **3** could be valuable for applications related to deep-blue emission. It is also found that elongation of the π-conjugated length could result in increased TPA cross sections, without a dramatic redshift of emission wavelength and low fluorescence quantum yield, probably due to the rigid planar structure of the chromophores.

Results and Discussion

Preparation of 1,8-Diazapyrenes

Synthesis of 1,8-diazapyrenes was concisely achieved by the coupling reaction of readily available 1,4-naphthoquinone *O*,*O*-diacetyl dioxime (**1**) with internal alkynes **2** under the $[\{RhCl_2Cp^*\}_2]$–$Cu(OAc)_2$ (Cp^* = pentamethylcyclopentadienyl ligand) bimetallic catalytic system, which has recently been developed in our group.[14] Treatment of a mixture of **1** and internal alkynes (2 equiv) with 5 mol% of $[\{RhCl_2Cp^*\}_2]$ and 20 mol% of $Cu(OAc)_2$ in *N*,*N*-dimethylformamide (DMF) at 60 °C resulted in concurrent formation of two pyridine rings through the sequence of *ortho*-aryl C–H bond cleavage, insertion of alkynes, and C–N bond formation, thereby giving the corresponding 1,8-diazapyrenes **3** (Table 1). While the reaction with 4-octyne (**2a**) gave 1,8-diazapyrene **3a** in the moderate yield (Table 1, entry 1), aryl alkynes such as **2b** and **2c** made the reactions smooth and afforded 1,8-diazapyrenes **3b** and **3c** in good yields (Table 1, entries 2 and 3). In the reaction with the asymmetrical alkyne 1-phenyl-1-propyne (**2d**) regioselective formation of 1,8-diazapyrene **3d** was observed in 59% yield (Table 1, entry 4). These 1,8-diazapyrenes are stable to air and moisture.

Table 1. One-step synthesis of 1,8-diazapyrenes **3**.[a]

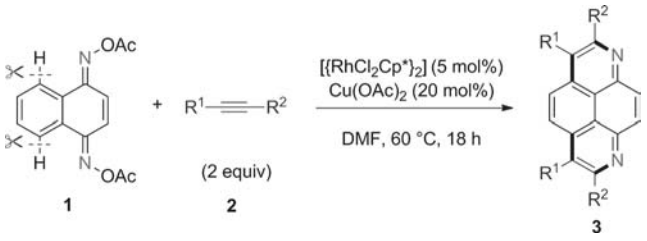

Entry	Alkynes	R^1	R^2	Yield of **3**[b] [%]
1	**2a**	*n*Pr	*n*Pr	33 (**3a**)
2	**2b**	Ph	Ph	72 (**3b**)
3	**2c**	4-Br-C_6H_4	4-Br-C_6H_4	71 (**3c**)
4	**2d**	Me	Ph	59 (**3d**)

[a] All reactions were carried out on a 0.5 mmol scale of oxime **1** with 2 equivalents of alkyne **2** under a nitrogen atmosphere. [b] Isolated yields based on oxime **1**.

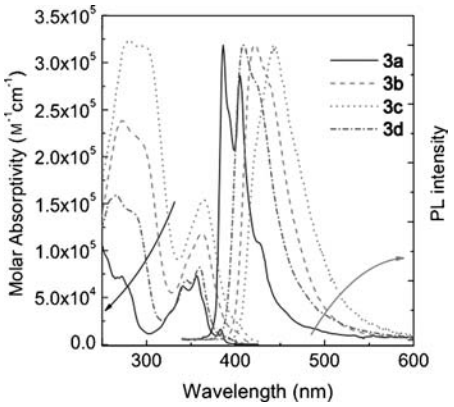

Figure 1. UV-visible and photoluminescence (PL) spectra of 1,8-diazapyrenes **3**.

One-Photon-Absorption and -Emission Properties

Figure 1 shows the UV-visible molar absorptivity spectra of chromophores **3a**, **3b**, **3c**, and **3d** in tetrahydrofuran (THF) at a concentration of 1.0×10^{-5} M L^{-1}. From the results shown in Figure 1, it can be observed that the one-photon-absorption and -emission spectra for chromophore **3a** exhibit a vibronic structure with the progression of several peaks; this indicates that there is a coupling with vibrational modes in chromophore **3a** that corresponds to C–C and/or C=C stretching during excitation from the ground state to the excited state, or the emission from the excited state down to the ground state. The absorption maximum of **3b** and **3c** is larger than those of **3a** and **3d** due to greater π conjugation. All of compounds **3** also show strong one-photon-excited PL spectra, which are comparatively shown in Figure 1. The emission peaks for chromophores **3a**, **3b**, **3c**, and **3d** are 405, 421, 442, and 410 nm, respectively, which are also in agreement with the order of the degree of π conjugation. The PL lifetime is an important parameter for organic emitting molecules, so we have also measured time-resolved PL (TRPL) decay curves for the four molecules (Figure 2). Compounds **3a**, **3b**, and **3d** have single-exponential PL emission decay behavior with lifetimes of 2.35, 3.55, and

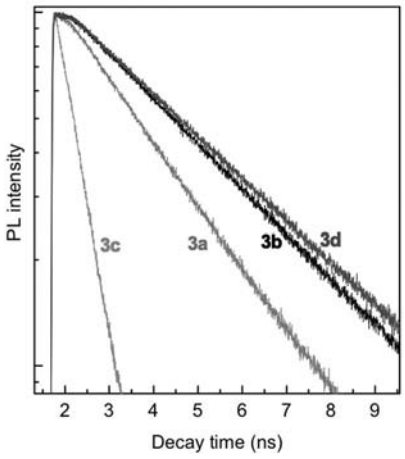

Figure 2. Room-temperature TRPL measurements of **3**.

Table 2. The lifetimes (τ) and fluorescence quantum yields (Φ_{PL}) for 1,8-diazapyrenes **3**.

	3a	3b	3c	3d
τ[a] [ns]	2.35	3.55	$\tau_2=1.57$ $\tau_1=0.48$	3.62
Φ_{PL}[b] [%]	4.5	2.7	1.9	4.5

[a] PL lifetime obtained from time-correlated single-photon counting (TCSPC). [b] Obtained by using quinine sulfate monohydrate ($\Phi=0.58$) as a standard.

3.62 ns, respectively, whereas the 4-bromophenyl adduct **3c** exhibits double-exponential PL decay behavior and a much faster decay rate, thus indicating a much stronger intermolecular interaction for **3c** in solution.[15] The shorter lifetime of **3a** can be attributed to a facile nonradiative decay pathway for this molecule, but this is much longer than that of many other organic molecules.[8,16,17] The long excited-state lifetimes of the compounds provide a major advantage for PL applications, such as diagnostics and optical amplification. The lifetimes (τ) and fluorescence quantum yield (Φ_{PL}) for the four compounds are summarized in Table 2.

TPA and Emission Properties

Note that all experimental results presented from here on correspond to intrinsic TPA cross sections measured in the femtosecond regime, and thereby, prevent contributions from linear nonresonant absorption or from excited-state absorption that may result in artificially enhanced TPA cross sections when the molecules are excited in the nanosecond regime.[18] It was found that **3a**, **3b**, **3c**, and **3d** showed strong two-photon-excited PL emission, which can be easily observed by the naked eye, as shown in Figure 3c. Figure 3b logarithmically shows the PL integrated intensity versus the excitation power of a 780 nm laser. All the plots have slopes near two, which coincides with the requirement for two-photon-excited PL.[1] To avoid the reabsorption effect due to high concentration of the molecules, the molecular solutions were freshly prepared at a concentration of 10^{-4} M L^{-1} in THF. In addition, the laser beam was focused as close as possible to the wall of the quartz cell and the PL signal was collected in back-scattering geometry, so that only the emission from the edge of the solution was collected. It was also found that TPA excited PL spectra for all of the compounds in THF were essentially the same as their one-photon-excited PL spectra, as shown in Figure 3a, thus implying that both one- and two-photon emissions were observed from the same excited state.

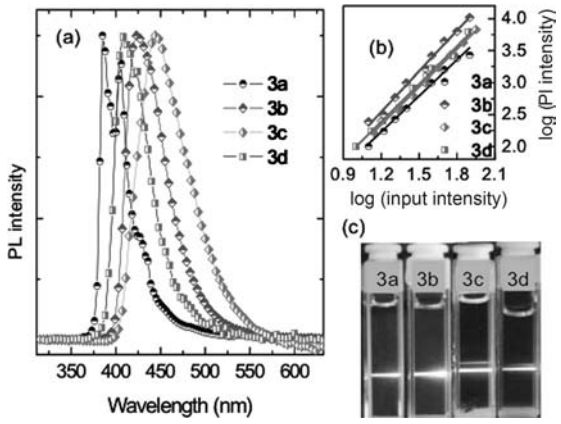

Figure 3. a) TPA excited PL spectra for **3**; b) PL integrated intensity versus power density at 780 nm. The log–log plots with slope values of around two indicate the nature of TPA in all of the compounds. c) Images of TPA excited PL emission for **3** under excitation at 780 nm.

To fully realize the potential application of two-photon excitation of the fluorescent molecules, it is important to know their TPA spectra. The TPA cross sections at a discrete wavelength for **3** were determined by the Z-scan method (Figure 4). By repeating the open-aperture Z-scan measurements for each laser wavelength, we can obtain the TPA spectra shown in Figure 5. Although chromophore **3a** exhibited small σ_2 values at excitation wavelengths, chromophores **3b–d** displayed much larger TPA cross sections. For example, the maximum σ_2 value of **3a** was 15 GM at 680 nm, whereas that of **3b** was around 120 GM at 680 nm. With the installation of 4-bromophenyl substituents (for **3c**), the maximum TPA cross section could be up to 298 GM at 800 nm, which was about 20 times larger than the maximum σ_2 of **3a**. Note that this value is even larger than all of the organic molecules reported in the literature.[11]

Although the quantum yields of **3** are lower than those of other compounds reported in the literature,[11] the TPA brightness values (the products of the peak TPA cross section and the fluorescence quantum yields) are still moderate due to their larger TPA cross sections, which are important for fluorescent molecule applications. It is known that the TPA process is a third-order nonlinear process, which is

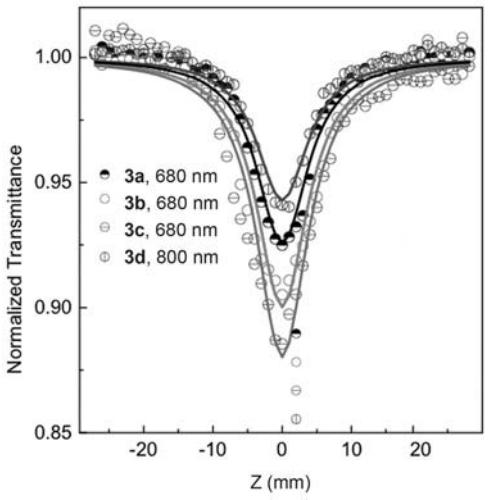

Figure 4. Open aperture Z-scan results for solutions of **3** obtained by using 680 or 800 nm femtosecond pulses (experimental data (open circles), theoretical fitted data (solid line)). The concentration of **3a** was 2×10^{-2} M and for the other three molecules was 2×10^{-3} M, excited with power densities of 277.1, 459.9, 226.0, and 411.5 GW cm^{-2}, giving a TPA coefficient of 0.0064, 0.0051, 0.0150, and 0.0035 cm GW^{-1} for **3a**, **3b**, **3c**, and **3d**, respectively.

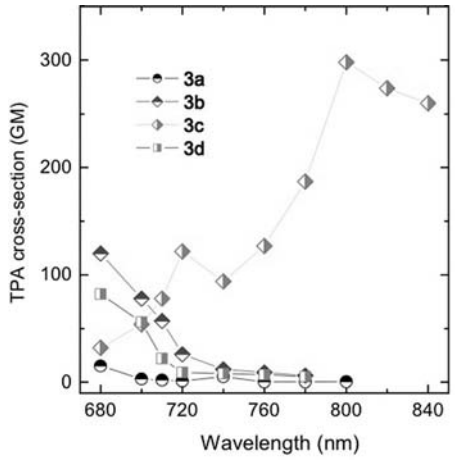

Figure 5. TPA spectra of 1,8-diazapyrenes **3** under the femtosecond pulse excitation.

strongly dependent on intramolecular charge transfer. The π-electron-rich substituents will induce an increase in charge transfer from the ends of the molecules to the center, resulting in larger σ_2 values. Therefore, compounds **3b**, **3c**, and **3d** exhibit much larger σ_2 values than those of **3a**. Note also that the maximum TPA coefficient of **3d** was five times larger than that of **3a**, without suffering from a dramatic redshift of emission wavelength and low fluorescence quantum yield. For **3a**, **3b**, and **3d**, the monotonic increase in TPA cross-section spectra at wavelengths below 800 nm indicates that the optimal excitation at wavelengths is shorter than the estimation based only on the linear absorption properties. This can be attributed to the higher electronic transition (S_0–S_n) for TPA excitation.[19] For centrosymmetric molecules, a three-level model can be utilized to describe their TPA properties, in which TPA into high-lying states is not dipole coupled to the ground state. It can be written as Equation (1):

$$\sigma_2 = \frac{M_{01}^2 M_{12}^2}{(E_1 - E_0 - \hbar\omega)^2 \Gamma} \quad (1)$$

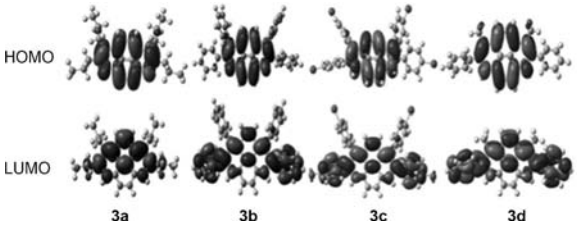

Figure 6. Geometry-optimized structural analyses of **3** for their HOMO and LUMO energies.

in which M_{01} and M_{12} are the transition dipole moments from S_0 to S_1 and S_1 to S_2, respectively; $\hbar\omega = (E_2 - E_0)/2$; and the damping factor, Γ, can be set to 0.1 V in almost all cases for the centrosymmetric molecules. The denominator is the square of the detuning energy between the ground and TPA states.[3,20] A smaller detuning energy will lead to a larger TPA cross section. From the TPA spectra presented in Figure 5, the detuning energy for **3c** is smaller than those for **3a**, **3b**, and **3d**. It is consistent with the much larger TPA cross sections for **3c**.

To evaluate the photostability of **3**, photobleaching experiments were performed for a solution of **3** in THF by using a power density of 100.01 GW cm^{-2} for 100 fs pulses at 780 nm. The emission intensities monitored at PL spectra peaks were recorded at time intervals of 5 s for a period of 1200 s. It was found that the emission intensities for all of the compounds decreased by less than 5%, which indicated the high photostability of **3**.

To gain an insight into the electronic structure of **3**, quantum chemical calculations were carried out by using the hybrid Hartree–Fock/DFT at the B3LYP/6-31G level.[21] The TPA cross section is related to the extent of intramolecular charge transfer through the π bridge in the molecule.[22] The HOMOs and LUMOs are depicted in Figure 6. From the calculated frontier orbitals, for **3a**, there are no changes on the localization of LUMO and HOMO. However, compared with the localization of HOMOs on the diazapyrene core, the LUMOs of **3b**, **3c**, and **3d** are delocalized on both the core and substituent, indicating an increase in intramolecu-

Table 3. The comparison of TPA cross-sectional values for **3** and other organic molecules with deep-blue emission.

Materials[a]	Methods[b]	λ_{ex} [nm]	σ_2 [GM]	λ_{abs} [nm]	λ_{em} [nm]	References
M-OPP(4)-SOR	TPEF, fs	600	31	319	407	[11a]
calix-OPP(4)-SOR	TPEF, fs	600	169	319	425	[11a]
1,4-bis(5,6-diphenyl-1,2,4-triazin-3-yl)benzene	NLT, fs	800	7	276	483	[11b]
1,3-bis(5,6-diphenyl-1,2,4-triazin-3-yl)benzene	NLT, fs	800	5	275	460	[11b]
2-[4-(1*H*-phenanthro[9,10-d]imidazol-2-yl)phenyl]benzoxazole	NLT, fs	800	21	376	461	[11b]
2-[4-(4,5-diphenyl-1*H*-imidazol-2-yl)phenyl]benzoxazole	NLT, fs	800	16	357	463	[11b]
2-styryl-1*H*-phenanthro[9,10-d]imidazole	NLT, fs	800	7	367	434	[11b]
trans-2-(*p*-formylstyryl)benzimidazole	TPEF, fs	750	180	270, 360	470	[11d]
3,7-bis[5′-(trifluoromethyl)-1′*H*-pyrazole-3′-yl]10-ethylphenothiazine	TPEF, fs	710	40	282, 336, 469	497	[11d]
3,7-bis[5′-(phenyl)-10*H*-pyrazole-3′-yl]10-ethylphenothiazine	TPEF, fs	710	59	278, 336, 458	494	[11d]
3a	Z scan	680	15	340, 356, 383,	386, 405[d]	this work
3b	Z scan	680	120	272, 296, 362	421[d]	this work
3c	Z scan	800	298	278, 300, 365, 403	442 nm[d]	this work
3d	Z scan	680	82	266, 286, 344, 359, 392	410[d]	this work

[a] The abbreviation of the materials is directly used from the corresponding reference. [b] PEF = two-photon-excited fluorescence method, NLT = nonlinear transmittance method. [d] Excited at 325 nm by using a continuous wave HeCd laser.

lar charge transfer and favoring the enhancement of their TPA cross sections. To facilitate the comparison, molecules reported with TPA cross sections with blue emission are listed in Table 3. Clearly, compounds **3b**, **3c**, and **3d** have larger TPA cross sections. In particular, compound **3c** has the largest maximum σ_2 of all other molecules in Table 3.

Conclusion

Efficient two-photon-excited emission in the deep-blue region has been demonstrated on newly synthesized 1,8-diazapyrenes **3** by pumping with femtosecond pulses. It was shown that the TPA cross section could be increased by elongation of the π conjugation of the 1,8-diazapyrenes **3** without a large redshift of the emission wavelength, which implied that varying the donors (or acceptors) linked to the 1,8-diazapyrene core was an effective way to tailor TPA properties for applications related to deep-blue emission. Our findings may open a new avenue to design highly efficient TPA molecules for blue PL emission and lasing as well as provide a novel series of organic molecules that can be used in nonlinear optical applications and fundamental studies.

Experimental Section

General

^{1}H NMR (400 MHz) spectra were recorded on a Bruker Avance 400 spectrometer in $CDCl_3$ (with $(CH_3)_4Si$ ($\delta = 0.00$ ppm) as an internal standard). ^{13}C NMR (100 MHz) spectra were recorded on a Bruker Avance 400 spectrometer in $CDCl_3$ (with residual $CHCl_3$ ($\delta = 77.00$ ppm) as an internal standard). The following abbreviations are used to explain the multiplicities: s = singlet, d = doublet, t = triplet, q = quartet, m = multiplet. IR spectra were recorded on a Shimazu IR Prestige-21 FTIR spectrometer. High-resolution mass spectra were obtained with a Finnigan MAT 95 XP mass spectrometer (Thermo Electron Corporation). Melting points were recorded on a Buchi B-54 melting-point apparatus. Flash column chromatography was performed by using Merck silica gel 60 with distilled solvents. Anhydrous DMF (99.8%), $Cu(OAc)_2$ (98% trace metal basis), Cu(OAc) (97%), and $[\{RhCl_2Cp^*\}_2]$ (97%) were purchased from Sigma–Aldrich.

*Preparation of (1E,4E)-Naphthalene-1,4-dione O,O-diacetyl dioxime (**1**)*

$NH_2OH{\cdot}HCl$ (1.32 g, 18.9 mmol) was added in one portion to a solution of naphthalene-1,4-dione (1.0 g, 6.3 mmol) and pyridine (2.5 mL, 31.5 mmol) in EtOH (6 mL) and the reaction mixture was stirred at 60 °C for 2 h. The reaction was quenched by adding water and the organic materials were extracted with CH_2Cl_2 (4×). The combined extracts were washed with 1 N aqueous HCl and brine, and dried over $MgSO_4$. Volatile materials were removed in vacuo to give (1*E*, 4*E*)-naphthalene-1,4-dione dioxime, which was used for the next acetylation step without further purification.

The crude residue obtained above was treated with Ac_2O (1.2 mL, 12.6 mmol) and a catalytic amount of 4-dimethylaminopyridine (DMAP; 5 mg) in pyridine (3 mL) and the reaction mixture was stirred at room temperature for 4 h. After the volatile materials were evaporated, the resulting residue was treated with water and organic materials were extracted in CH_2Cl_2 (4×). The combined extracts were washed with 1 N aqueous HCl and brine and dried over $MgSO_4$. The solvents were removed under reduced pressure and the crude was purified by silica-gel flash column chromatography (*n*-hexane/ethyl acetate = 60:40) to yield oxime **1** as a reddish brown solid (0.51 g, 1.89 mmol, 30%). M.p. 146–148 °C; ^{1}H NMR (400 MHz, $CDCl_3$): $\delta = 2.36$ (6H, s), 7.55 (2H, s), 7.56 (2H, dd, $J = 3.6$, 6.4 Hz), 8.37 ppm (2H, dd, $J = 3.6$, 6.0 Hz); ^{13}C NMR (100 MHz, $CDCl_3$): $\delta = 19.8$, 122.2, 124.3, 128.5, 130.9, 150.8, 168.2 ppm; IR (NaCl) 1773, 1620, 1574, 1539, 1520, 1368, 1188, 939 cm^{-1}; HRMS (ESI): *m*/*z* calcd for $C_{14}H_{13}N_2O_4$: 273.0875 $[M+H]^+$; found: 273.0884.

*Synthesis of 1,8-Diazapyrene **3***

A typical procedure for the reaction of **1** and **2b** (Table 1, entry 2): $[\{RhCl_2Cp^*\}_2]$ (15.5 mg, 0.025 mmol) and $Cu(OAc)_2$ (18.2 mg, 0.20 mmol) were added to a solution of **1** (136.1 mg, 0.50 mmol) and **2b** (178.2 mg, 1.00 mmol) in DMF (1.5 mL) and the reaction mixture was stirred at 60 °C under a nitrogen atmosphere for 18 h. After being cooled to room temperature, the reaction was quenched with pH 9 buffer and organic materials were extracted with CH_2Cl_2 (3×). The combined extracts were washed with water (3×) and brine and dried over $MgSO_4$. The solvents were removed under reduced pressure and the crude was purified by silica-gel flash column chromatography (*n*-hexane/ethyl acetate = 80:20) to afford **3b** as an orange solid (92.4 mg, 0.286 mmol, 72%). M.p. 275–277 °C; ^{1}H NMR (400 MHz, $CDCl_3$): $\delta = 7.28$–7.34 (m, 10H), 7.36–7.41 (m, 6H), 7.51–7.54 (m, 4H), 8.04 (s, 2H), 8.70 ppm (s, 2H); ^{13}C NMR (100 MHz, $CDCl_3$): $\delta = 117.2$, 127.58, 127.60, 127.8, 128.2, 129.0, 130.5, 130.7, 131.6, 133.0, 134.4, 136.9, 140.9, 147.3, 156.2 ppm; IR (NaCl): $\tilde{\nu} =$ 1557, 1445, 1381, 1074, 1030 cm^{-1}; HRMS (ESI): *m*/*z* calcd for $C_{38}H_{25}N_2$: 509.2018 $[M+H]^+$; found: 509.2018.

*2,3,6,7-Tetrapropylbenzo[lmn][2,9]phenanthroline (**3a**)*

Brownish red solid; M.p. 77–78 °C; ^{1}H NMR (400 MHz, $CDCl_3$): $\delta = 1.13$ (t, $J = 7.2$ Hz, 6H), 1.16 (t, $J = 7.2$ Hz, 6H), 1.76–1.85 (m, 4H), 1.92–2.01 (m, 4H), 3.23–3.27 (m, 4H), 3.28–3.33 (m, 4H), 8.39 ppm (s, 4H); ^{13}C NMR (100 MHz, $CDCl_3$): $\delta = 14.5$, 14.6, 24.0, 25.2, 30.2, 38.3, 117.3, 126.4, 128.8, 131.3, 133.1, 145.7, 158.4 ppm; IR (NaCl): $\tilde{\nu} = 2961$, 2932, 2872, 1562, 1477, 1456, 1391, 1263 cm^{-1}; HRMS(ESI): *m*/*z* calcd for $C_{26}H_{33}N_2$: 373.2644 $[M+H]^+$; found: 373.2645.

*2,3,6,7-Tetrakis(4-bromophenyl)benzo[lmn][2,9]phenanthroline (**3c**)*

Yellowish green solid; M.p. 191–193 °C; ^{1}H NMR (400 MHz, $CDCl_3$): $\delta =$ 7.20 (d, $J = 8.0$ Hz, 4H), 7.39 (d, $J = 8.4$ Hz, 4H), 7.47 (d, $J = 8.4$ Hz, 4H), 7.58 (d, $J = 8.0$ Hz, 4H), 8.01 (s, 2H), 8.67 ppm (s, 2H); ^{13}C NMR (100 MHz, $CDCl_3$): $\delta = 117.1$, 122.4, 122.6, 128.9, 129.3, 131.3, 131.8, 132.1, 133.1, 133.3, 134.2, 135.5, 139.5, 147.7, 154.9 ppm; IR (NaCl): $\tilde{\nu} =$ 1587, 1549, 1491, 1377, 1126, 1070, 1011, 833 cm^{-1}; HRMS (ESI): *m*/*z* calcd for $C_{38}H_{21}N_2{}^{79}Br_2{}^{81}Br_2$: 824.8397 $[M+H]^+$; found: 824.8403.

*3,6-Dimethyl-2,7-diphenylbenzo[lmn][2,9]phenanthroline (**3d**)*

Yellow solid; M.p. 234–236 °C; ^{1}H NMR (400 MHz, $CDCl_3$): $\delta = 2.94$ (s, 6H), 7.48–7.52 (m, 2H), 7.56–7.60 (m, 4H), 7.71–7.74 (m, 4H), 8.52 (s, 2H), 8.53 ppm (s, 2H); ^{13}C NMR (100 MHz, $CDCl_3$): $\delta = 16.1$, 117.2, 124.3, 126.9, 128.0, 128.3, 129.8, 132.1, 134.2, 141.5, 146.0, 157.5 ppm; IR (NaCl): $\tilde{\nu} = 3057$, 2968, 1558, 1474, 1379, 1362, 1016, 833 cm^{-1}; HRMS (ESI): *m*/*z* calcd for $C_{28}H_{21}N_2$: 385.1705 $[M+H]^+$; found: 385.1705.

Optical Absorption and Emission Spectra

Linear absorption spectra for compounds **3** were recorded on a Shimadzu UV-3101 PC spectrophotometer. For the one-photon-excited PL, a continuous wave HeCd laser emitting at 325 nm was used as the excitation source and the signal was dispersed by a 750 mm monochromator combined with suitable filters, and detected by a photomultiplier using the standard lock-in amplifier technique.

TPA Cross-Sectional Measurements

TPA coefficients of molecules were measured by using the Z-scan technique.[13] The compounds were dissolved in THF and placed in 1 mm quartz cuvettes. The laser source is a Ti:sapphire system that produced 100 fs (HW1/e) pulses at a repetition of 80 MHz. Measurements were carried out in the wavelength range of 680–820 nm for TPA excitation. In the measuring process, the input laser beam was first passed though

a beam chopper with an open ratio of 1/10 and a rotating speed of 315 rounds per second. Then the Gaussian beam was tightly focused onto the samples by a convex lens ($f=10$ cm). The transmitted beam was detected by a silicon photodiode using the standard lock-in amplifier technique. The measured curves were symmetric with respect to the focal point ($z=0$), where they exhibit a minimum transmittance in the case of TPA. The TPA coefficient, β, can be estimated from the normalized transmittance given by Equation (2):

$$T_{OA(TPA)} = \frac{1}{1+\beta L_{eff}[I_{00}/(1+(z/z_0)^2)]} \quad (2)$$

in which I_{00} is the peak intensity, z is the sample position, $z_0 = \pi\omega_0^2/\lambda$ is the diffraction length of the beam, ω_0 is the beam waist radius at the focus point, and $L_{eff}=[1-\exp(-\alpha_0 L)]/\alpha_0$ is the effective thickness of the sample. As a macroscopic parameter that depends on the concentration of the TPA molecules, β (in units of $cm\,GW^{-1}$) can be further expressed as $\beta=\sigma_2' N_0=\sigma_2' N_A d_0\times 10^{-3}$, in which σ_2' is the molecular TPA cross section (in units of $cm^4 GW^{-1}$), N_0 is the molecular density (in units of cm^{-3}), N_A is Avogadro's number, and d_0 is the molar concentration of the absorbing molecules (in units of $M\,L^{-1}$). Moreover, one can also use another parallel expression for the TPA cross section, defined as $\sigma_2 = h\nu\sigma_2'$, in which $h\nu$ is the photon energy of the input light beam. According to this definition, σ_2 can be calculated in units of GM.[23]

Acknowledgements

Support from the Singapore Ministry of Education through the Academic Research Fund (Tier 1) under Project No. RG63/10 (for S.H.D.), from the Singapore National Research Foundation through the Competitive Research Programme (CRP) under Project No. NRF-CRP5-2009-04 (for S.H.D.), and from the Science & Engineering Research Council for A*STAR Grant No. 082 101 0019 (for C.S.) is gratefully acknowledged. We thank Prof. Changshun Wang from Shanghai Jiao Tong University for providing us with the Z-scan measurement system and for helpful discussions.

[1] G. S. He, L. Tan, Q. Zheng, P. N. Prasad, *Chem. Rev.* **2008**, *108*, 1245–1330.

[2] a) B. A. Reinhardt, L. L. Brott, S. J. Clarson, A. G. Dillard, J. C. Bhatt, R. Kannan, L. Yuan, G. S. He, P. N. Prasad, *Chem. Mater.* **1998**, *10*, 1863–1874; b) R. Kannan, G. S. He, L. Yuan, F. Xu, P. N. Prasad, A. G. Dombroskie, B. A. Reinhardt, J. W. Baur, R. A. Vaia, L.-S. Tan, *Chem. Mater.* **2001**, *13*, 1896–1904; c) L. Beverina, J. Fu, A. Leclercq, E. Zojer, P. Pacher, S. Barlow, E. W. Van Stryland, D. J. Hagan, J. L. Brédas, S. R. Marder, *J. Am. Chem. Soc.* **2005**, *127*, 7282–7283.

[3] M. Albota, D. Beljonne, J. L. Brédas, J. E. Ehrlich, J. Y. Fu, A. A. Heikal, S. E. Hess, T. Kogej, M. D. Levin, S. R. Marder, D. McCord-Maughon, J. W. Perry, H. Röckel, M. Rumi, G. Subramaniam, W. W. Webb, X. L. Wu, C. Xu, *Science* **1998**, *281*, 1653–1656.

[4] D. Beljonne, W. Wenseleers, E. Zojer, Z. Shuai, H. Vogel, S. J. K. Pond, J. W. Perry, S. R. Marder, J. L. Brédas, *Adv. Funct. Mater.* **2002**, *12*, 631–641.

[5] a) K. Ogawa, A. Ohashi, Y. Kobuke, K. Kamada, K. Ohta, *J. Am. Chem. Soc.* **2003**, *125*, 13356–13357; b) T. K. Ahn, K. S. Kim, D. Y. Kim, S. B. Noh, N. Aratani, C. Ikeda, A. Osuka, D. Kim, *J. Am. Chem. Soc.* **2006**, *128*, 1700–1704; c) S. Saito, J. Y. Shin, J. M. Lim, K. S. Kim, D. Kim, A. Osuka, *Angew. Chem.* **2008**, *120*, 9803–9806; *Angew. Chem. Int. Ed.* **2008**, *47*, 9657–9660.

[6] a) C. Katan, S. Tretiak, M. H. V. Werts, A. J. Bain, R. J. Marsh, N. Leonczek, N. Nicolaou, E. Badaeva, O. Mongin, M. Blanchard-Desce, *J. Phys. Chem. B* **2007**, *111*, 9468–9483; b) M. Williams-Harry, A. Bhaskar, G. Ramakrishna, T. Goodson III, M. Imamura, A. Mawatari, K. Nakao, H. Enozawa, T. Nishinaga, M. Iyoda, *J. Am. Chem. Soc.* **2008**, *130*, 3252–3253; c) A. Fukazawa, H. Yamada, Y. Sasaki, S. Akiyama, S. Yamaguchi, *Chem. Asian J.* **2010**, *5*, 466–469.

[7] Y. Zhang, S. L. Lai, Q. X. Tong, M. F. Lo, T. W. Ng, M. Y. Chan, *Chem. Mater.* **2012**, *24*, 61–70.

[8] a) D. Schneider, T. Rabe, T. Riedl, T. Dobbertin, M. Kröger, E. Becker, H.-H. Johannes, W. Kowalsky, T. Weimann, J. Wang, P. Hinze, A. Gerhard, P. Stössel, H. Vestweber, *Adv. Mater.* **2005**, *17*, 31–34; b) T. C. He, R. Chen, W. W. Lin, F. Huang, H. D. Sun, *Appl. Phys. Lett.* **2011**, *99*, 081902–081904.

[9] Z. Zeng, Z. Guan, Q. Xu, J. Wu, *Chem. Eur. J.* **2011**, *17*, 3837–3841.

[10] Q. Zheng, S. K. Gupta, G. S. He, L. S. Tan, P. N. Prasad, *Adv. Funct. Mater.* **2008**, *18*, 2770–2779.

[11] a) H. H. Fan, K. F. Li, X. L. Zhang, W. Yang, M. S. Wong, K. W. Cheah, *Chem. Commun.* **2011**, *47*, 3879–3881; b) Y. Sun, W. Huang, C. Lu, Y. Cui, *Dyes Pigm.* **2009**, *81*, 10–17; c) Z. L. Huang, N. Li, H. Lei, Z. R. Qiu, H. Z. Wang, Z. P. Zhong, Z. H. Zhou, *Chem. Commun.* **2002**, 2400–2401; d) D. M. Li, L. Lv, P. Sun, W. Zhou, P. Wang, J. Wu, Y. Kan, H. Zhou, Y. Tian, *Dyes Pigm.* **2009**, *83*, 180–186.

[12] H. C. Becker, A. Broo, B. Norden, *J. Phys. Chem. A* **1997**, *101*, 8853–8860.

[13] M. Sheik-Bahae, A. A. Said, T. H. Wei, D. J. Haga, E. W. Van Stryland, *IEEE J. Quantum Electron.* **1990**, *26*, 760–769.

[14] a) P. C. Too, S. H. Chua, S. H. Wong, S. Chiba, *J. Org. Chem.* **2011**, *76*, 6159–6168; b) Y. F. Wang, K. K. Toh, J. Y. Lee, S. Chiba, *Angew. Chem.* **2011**, *123*, 6049–6053; *Angew. Chem. Int. Ed.* **2011**, *50*, 5927–5931; c) P. C. Too, T. Noji, Y. J. Lim, X. Li, S. Chiba, *Synlett* **2011**, 2789–2794; d) P. C. Too, Y. F. Wang, S. Chiba, *Org. Lett.* **2010**, *12*, 5688–5691.

[15] G. S. He, Q. Zheng, C. Lu, P. N. Prasad, *IEEE J. Quantum Electron.* **2005**, *41*, 1037–1043>.

[16] B. Xu, H. Fang, F. Chen, H. Lu, J. He, Y. Li, Q. Chen, H. Sun, W. Tian, *New J. Chem.* **2009**, *33*, 2457–2464.

[17] T. B. Clark, M. E. Orr, D. C. Flynn, T. Goodson III, *J. Phys. Chem. C* **2011**, *115*, 7331–7338.

[18] R. L. Sutherland, M. C. Brant, J. Heinrichs, J. E. Rogers, J. E. Slagle, D. G. McLean, P. A. Fleitz, *J. Opt. Soc. Am. B* **2005**, *22*, 1939–1948.

[19] M. Drobizhev, N. S. Makarov, S. E. Tillo, T. E. Hughes, A. Rebane, *Nat. Methods* **2011**, *8*, 393–399.

[20] S. Chung, S. Zheng, T. Odani, L. Beverina, J. Fu, L. A. Padilha, A. Biesso, J. M. Hales, X. Zhan, K. Schmidt, A. Ye, E. Zojer, S. Barlow, D. J. Hagan, E. W. Van Stryland, Y. Yi, Z. Shuai, G. A. Pagani, J. Brédas, J. W. Perry, S. R. Marder, *J. Am. Chem. Soc.* **2006**, *128*, 14444–14445.

[21] Gaussian 98, M. J. Frisch, G. W. Trucks, H. B. Schlegel, G. E. Scuseria, M. A. Robb, J. R. Cheeseman, V. G. Zakrzewski, J. A. Montgomery, Jr., R. E. Stratmann, J. C. Burant, S. Dapprich, J. M. Millam, A. D. Daniels, K. N. Kudin, M. C. Strain, O. Farkas, J. Tomasi, V. Barone, M. Cossi, R. Cammi, B. Mennucci, C. Pomelli, C. Adamo, S. Clifford, J. Ochterski, G. A. Petersson, P. Y. Ayala, Q. Cui, K. Morokuma, P. Salvador, J. J. Dannenberg, D. K. Malick, A. D. Rabuck, K. Raghavachari, J. B. Foresman, J. Cioslowski, J. V. Ortiz, A. G. Baboul, B. B. Stefanov, G. Liu, A. Liashenko, P. Piskorz, I. Komaromi, R. Gomperts, R. L. Martin, D. J. Fox, T. Keith, M. A. Al-Laham, C. Y. Peng, A. Nanayakkara, M. Challacombe, P. M. W. Gill, B. Johnson, W. Chen, M. W. Wong, J. L. Andres, C. Gonzalez, M. Head-Gordon, E. S. Replogle, J. A. Pople, Gaussian, Inc., Pittsburgh, PA, **1998**.

[22] V. Chandrasekhar, M. D. Pandey, S. K. Maurya, P. Sen, D. Goswami, *Chem. Asian J.* **2011**, *6*, 2246–2250.

[23] G. S. He, C. Xu, P. N. Prasad, B. A. Reinhardt, J. C. Bhatt, A. G. Dillard, *Opt. Lett.* **1995**, *20*, 435–437.

Received: February 21, 2012
Published online: June 14, 2012

